Grouping Line-segments using Eigenclustering

Antonio Robles Kelly(*) and Edwin R. Hancock(†)
Department of Computer Science,
University of York, York Y01 5DD, UK
arobkell@cs.york.ac.uk(*) erh@cs.york.ac.uk(†)

Abstract

This paper presents an eigenclustering approach to line-segment grouping. We make three contributions. First, we show how the geometry of the line-endpoints can be used to compute a grouping field by interpolating a polar lemniscate between them. Second, we show how to adaptively threshold the grouping field to produce a line-adjacency matrix. Finally, we present a non-iterative method for locating line-groupings using the eigenvectors of the adjacency matrix.

1 Introduction

Line-segment grouping is a crucial task in intermediate level vision. The reasons for this are two-fold. Firstly, edge detection is an inherently unreliable process which results in segmentation errors such as line fragmentation or corner dropout. Before significant structures can be extracted, then these errors must be corrected. Secondly, the significant perceptual groupings may be subsumed in clutter or background. The goal of line grouping is to extract significant perceptual structure from background while correcting line-fragmentation errors.

The line grouping process can be viewed as a three-stage process. First, the geometry of adjacent line-segment pairs is used to compute a grouping field which gauges their perceptual affinity to one-another. There are a number of ways in which this can be done. For instance, several authors including Guy and Medioni [2] and ShaShua and Ullman [8] have used curvature criteria to group edgels. Heitger and von der Heydt [3] have a biologically plausible grouping field based on polar alignment potentials. Jacobs and Williams have developed a stochastic completion field [13][12]. Once the grouping field is to hand, then the next task is to compute a perceptual adjacency graph by thresholding the grouping field. Finally, perceptual groupings can be extracted from the grouping field or the adjacency graph. One of the most popular approaches here is to use the eigenstructure of the adjacency graph to find the main groupings. This can be viewed as using pairwise clustering to to find significant arrangements for instance Perona and Freeman [5] extend the iterative normalised cut idea of Shi and Malik [9] to line-patterns. Sarkar and Boyer [7] have used ideas from spectral graph theory to find disjoint subgraphs of the line-adjacency matrix. However, this method is again an iterative one since it requires each cluster in turn to be located and removed from the scene.

Our aims in this paper are threefold. First, we aim to show how ideas similar to those of Heitger and von der Heydt [3] can be used to compute a grouping field for line-segments. Rather than using polar kernels to accumulate a grouping field for individual

BMVC 2000 doi:10.5244/C.14.59

edgels, we use them to model the grouping of lines using the geometry of their endpoints. Second, we show how to adaptively threshold the resulting grouping field to produce a line-adjacency matrix. Finally, we develop a non-iterative method for simultaneously extracting all of the perceptual clusters from the line-adjacency matrix. We provide a theoretical analysis which demonstrates that the perceptual clusters can be extracted simulataneously using the different eigenvectors.

2 Probabilistic Grouping Field

We are interested in locating groups of line-segments that exhibit strong geometric affinity to one-another. In this section we provide details of a probabilistic linking field that can be used to gauge geometric affinity. To be more formal suppose we have a set of line-segments $\mathcal{L} = \{\Lambda_i; i = 1, ..., n\}$. Consider two lines Λ_i and Λ_j drawn from this set. Their respective lengths are l_i and l_j. Our model of the linking process commences by constructing the line $\Gamma_{i,j}$ which connects the closest pair of endpoints for the two lines. The geometry of this connecting line is represented using the polar angle θ_{ij} of the line $\Gamma_{i,j}$ with respect to the base-line Λ_i and its ρ_{ij}. We measure the overall scale of the arrangement of lines using the length of the shorter line $\hat{\rho}_{i,j} = \min[l_i, l_j]$.

The relative length of the gap between the two line-segments is represented in a scale-invariant manner using the dimensionless quantity $\zeta_{i,j} = \frac{\rho_{i,j}}{\hat{\rho}_{i,j}}$.

Following Heitger and Von der Heydt [3] we model the linking process using an elongated polar grouping field. To establish the degree of geometric affinity between the lines we interpolate the end-points of the two lines using the polar lemniscate

$$\zeta_{i,j} = k \cos^2 \theta_{i,j} \tag{1}$$

The value of the constant k is used to measure the degree of affinity between the two lines. For each linking line, we compute the value of the constant k which allows the polar locus to pass through the pair of endpoints. The value of this constant is

$$k = \frac{\rho_{i,j}}{\hat{\rho}_{i,j} \cos^2 \theta_{i,j}} \tag{2}$$

The geometry of the lines and their relationship to the interpolating polar lemniscate is illustrated in Figure 1. It is important to note that the polar angle is defined over the interval $\theta_{ij} \in (-\pi/2, \pi/2]$ and is rotation invariant.

We use the parameter k to model the linking probability for the pair of line-segments. When the lemniscate envelope is large, i.e. k is large, then the grouping probability is small. On the other hand, when the envelope is compact, then the grouping probability is large. To model this behaviour, we assign the linking probability using the exponential distribution

$$P_{ij} = \exp[-\lambda k] \tag{3}$$

where λ is a constant whose best value has been found empirically to be unity. As a result, the linking probability is large when either the relative separation of the endpoints is small i.e. $\rho_{i,j} << \hat{\rho}_{i,j}$ or the polar angle is close to zero or π, i.e. the two lines are colinear or parallel. The linking probability is small when either the relative separation of the endpoints is large i.e. $\rho_{i,j} >> \hat{\rho}_{i,j}$ or the polar angle is close to $\frac{\pi}{2}$, i.e. the two lines are perpendicular. In Figure 2 we show a plot of the linking probability as a function of $\frac{\rho_{i,j}}{\hat{\rho}_{i,j}}$ and $\theta_{i,j}$.

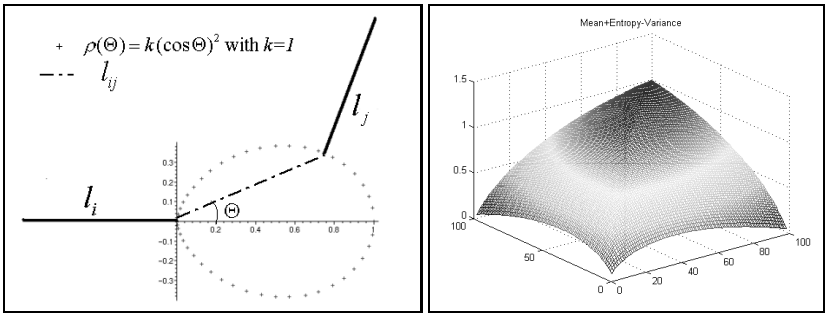

(a) (b)

Figure 1: (a) Geometric meaning of the parameters used to obtain P_{ij}; (b) 3D plot showing the threshold for all the combinations of a_{ij} with $n = 2$

2.1 The Entropy Based Thresholding

With the linking field to hand, we can construct a binary line-adjacency matrix. The elements $A_{i,j}$ of the matrix are computed by thresholding the linking probabilities using the following rule

$$A_{ij} = \begin{cases} 1 & \text{if } P_{ij} \geq \epsilon \text{ and } i \neq j \\ 0 & \text{if } i = j \\ 0 & \text{otherwise} \end{cases} \quad (4)$$

The threshold ϵ is computed using the mean, variance and entropy of the linking probabilities. However, prior to computing these quantities, we set to zero all elements

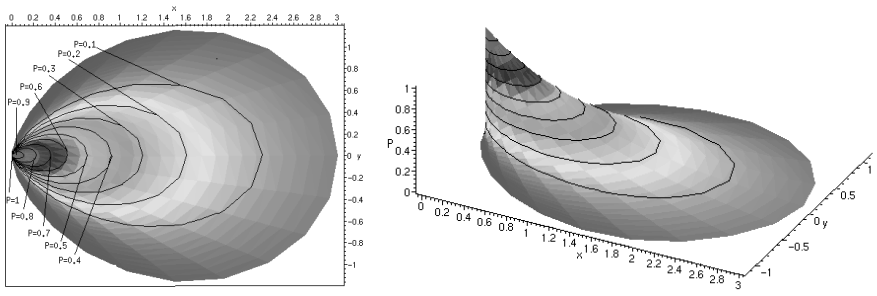

(a) (b)

Figure 2: (a) Plot showing the level curves; (b) 3D plot showing P_{ij} on the z axis

of the matrix A whose elements are vanishingly small. If there are N non-vanishing elements of the matrix A, then the mean, variance and entropy are defined as follows

$$\mu = \frac{1}{N}\sum_{i=1}^{n}\sum_{j=1}^{n} P_{ij} \tag{5}$$

$$\sigma^2 = \frac{1}{N}\sum_{i=1}^{n}\sum_{j=1}^{n} (\mu - P_{ij})^2 \tag{6}$$

$$h = -\frac{1}{N}\sum_{i=1}^{n}\sum_{j=1}^{n} P_{i,j}\log_2 P_{ij} \tag{7}$$

The mean and variance measure the average value and the spread of the linking probabilities. The entropy measures the degree of equivocation or ambiguity. We set the threshold to be

$$\epsilon = \mu - \sigma + h \tag{8}$$

In this way the threshold is large if either the variance is large or the entropy is large, i.e. there is a high degree of equivocation concerning the adjacency of a line-segment. The idea of using the entropy to set the threshold is widespread in the literature on binary image segmentation. Thorough reviews of the topic can be found in [11] and [6]. In Fig. 1(b) we a 3D plot of the threshold ϵ as a function of the linking probability P.

2.2 The Eigenclustering Process

The overall aim in this paper is to demonstrate that perceptual groupings can be extracted from line-patterns using the eigen-modes of the line-adjacency matrix A. There are many variants of this idea described in the computer literature. For instance, the closely related algorithms of Perona and Freeman [5], and, Sarkar and Boyer [7] both use the first eigenvalue to locate groupings. Shi and Malik [9], on the other hand, have used the second smallest eigenvalue to segment the image into background and foreground using the iterative normalised cut method.

Stated formally, the problem is as follows. If a scene consists of distinct groups of line-segments, then each grouping can be represented by a disjoint adjacency graph. Suppose that each of the disjoint adjacency graphs G_i are represented by the adjacency matrices B_i. If the overall scene is represented by an adjacency matrix A, then the identification of the disjoint adjacency graphs can be posed as that of locating the permutation matrix Q which transforms the adjacency matrix A into a block-diagonal matrix B whose submatrices are B_i. The block diagonal matrix satisfies the condition $B = QAQ^T$. There are many ways of recovering the permutation matrix Q. Here we use the method of characteristic polynomials.

To develop our eigenclustering method we make use of several results from linear algebra and spectral graph theory [1]:

- **Theorem 1:** Consider the direct sum of m graphs $G_1, \ldots, G_m$. Let B_i be the adjacency matrix of the graph $G_i (i = 1, \ldots, m)$. The adjacency matrix B of $G_1 + \ldots + G_m$ is of the form:

$$B = \begin{pmatrix} B_1 & \ldots & O \\ \vdots & \ddots & \vdots \\ O & \ldots & B_m \end{pmatrix} \tag{9}$$

Further, let $R_B(\lambda)$ be the characteristic polynomial of the eigenvalue equation $\mid B - \lambda I \mid = 0$. If a graph is the direct sum of the m components $B_l, l \in (1, \ldots, m)$ then:

$$R_B(\lambda) = R_{B_1}(\lambda) \cdots R_{B_m}(\lambda) \tag{10}$$

This property can be demonstrated using the Laplace expansion of the determinant.

We will also use the following theorem from [10]:

- **Theorem 2:** Let B_i be an n by n irreducible non-negative block matrix with distinct eigenvalues $\lambda_1, \ldots, \lambda_n$, then there exists an eigenvector x associated with $\alpha = max(\lambda_1, \ldots, \lambda_n)$ whose coefficients are all positive.

From the theory of linear equations we can derive the following theorem:

- **Theorem 3:** Suppose that the adjacency matrix B of $G_1 + \ldots + G_m$ is of the block-diagonal form:

$$B = \begin{pmatrix} B_1 & \ldots & O \\ \vdots & \ddots & \vdots \\ O & \ldots & B_m \end{pmatrix} \tag{11}$$

  Since the eigenvalues of B are the union of the eigenvalues of $G_1, \ldots, G_m$ then if there exists a $\lambda_j \in R_{B_i}(\lambda), i = (1, 2, \ldots, m)$ with multiplicity 1, then there exists an eigenvector $\underline{\mathrm{x}}(\lambda_j)$ corresponding to λ_j whose coefficients corresponding to the nodes in G_l with $l \neq i$ and $l = (1, 2, \ldots, m)$ are null.

We can use these properties to locate the distinct perceptual clusters, or subgraphs, in the line-pattern adjacency matrix. Our goal is to find the permutation matrix Q which induces a block diagonal structure on the matrix A. The blocks are associated with the eigenvectors whose eigenvalues are positive and whose components are all of the same sign. To be more formal, let the set of eigenvectors of A be $S = \{\underline{\mathrm{x}}(\lambda_j) \mid j = 1, 2, \ldots, n\}$, where $\underline{\mathrm{x}}(\lambda_j) = (x_1(\lambda_j), x_2(\lambda_j), \ldots, x_n(\lambda_j))^T$ is the eigenvector of A associated with the eigenvalue λ_j. Using the theorems listed above the eigenmodes associated with the clusters are those which have positive eigenvalues ($\lambda_j > 0$) and whose eigenvectors all have components of the same sign ($x_i(\lambda_1) > 0 \; \forall \; i$ or $x_i(\lambda_j) < 0 \; \forall \; i$).

Another important consequence of this property is that the first eigenvalue of the matrix A will describe the graph G_i. As a result the most significant cluster can be identified by choosing only the first eigenvalue of A. It should be noted that the eigenvectors obtained describe only the clusters with more than one member. This is a useful property, since it allows us to discard noise.

These properties allow us to develop a single-pass clustering algorithm. We assign nodes to clusters in the following way. First, we follow Theorem 2 and select the eigenvectors which have positive eigenvalues. Next, we select those eigenvectors whose coefficients are all either of the same sign, or are zero, as cluster prototypes. The node i is assigned to the cluster with eigenvalue λ_j provided that $x_i(\lambda_j) > 0$. Because the eigenvalues are unique from Theorem 3 this results in an unambiguous assignment.

2.3 Pseudocode

Now that we have presented the theoretical basis of the algorithm, we can develop a practical algorithm for assigning lines to eigenclusters and hence extract perceptual groupings. The pseudo-code for the algorithm is listed below.

```
For i = 1, 2, ..., n
    For j = 1, 2, ..., n
        Get P_ij;
For i = 1, 2, ..., n
    For j = 1, 2, ..., n
        Get A_ij;
Get the eigenvalues λ_1, λ_2, ..., λ_n of A;
Get the eigenvectors x(λ_1), x(λ_1), ..., x(λ_n) of A;
m = 0;
For i = 1, 2, ..., n
    {
    k = 0; l = 0;
    If λ_i > 0 then
        For j = 1, 2, ..., n
        {
            If x_j(λ_i) ≥ 0 then k = k + 1;
            If x_j(λ_i) ≤ 0 then l = l + 1;
        }
    If k = n or l = n then
        {
        m = m + 1;
        For j = 1, 2, ..., n
            If x_j(λ_i) ≠ 0 then Node_j ∈ Cluster_m;
        }
    }
```

3 Experiments

We have experimented with the new line-grouping method on three types of data. These are artificial text patterns, patterns extracted from synthetic images and line-patterns extracted from real-world images. These experiments will be described in more detail in the remainder of this section

3.1 Test Patterns

Our aim here is to test the response of the grouping field under varying opening angle, gap lengths and relative line-lengths. We present our results using the opening angle $\theta_{i,j}$ and the normalised length $\zeta_{i,j} = \frac{\rho_{i,j}}{\hat{\rho}_{i,j}}$.

Our test patterns are composed of 7 straight lines arranged in a concentric way. The distance between the center of the pattern and the starting point of each line is identical. However, we have varied the length of the gap. Since the linking field is symmetric, for the purposes of testing it is sufficient to vary the angles of the lines in the patterns from 0 to 2π in intervals of $\pi/2$.

In Figure 3 we show two examples of the test-pattern with different gap-lengths. In Figure 4 we show plots of the linking probability $P_{i,j}$ (left) and the normalised gap-length $\zeta_{i,j}$ for the two patterns. θ_{ij}. The quantities are computed with respect to the base-line l_0. The x-axis of the plots is the line-index of the lines in the figure. The plots show that the linking field is weak when the curvature of the line segment pair is large.

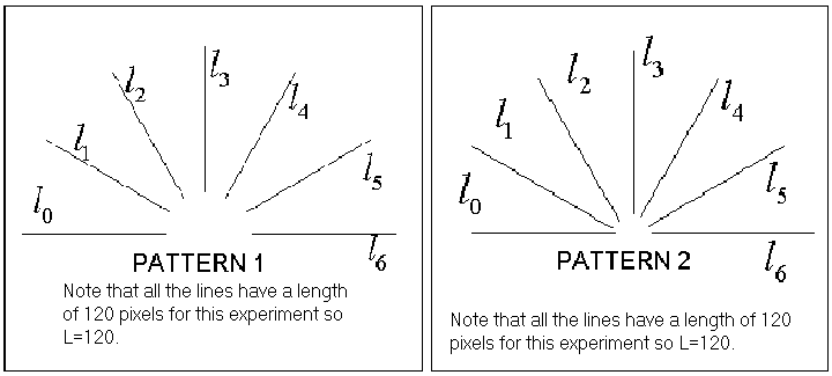

Figure 3: Test patterns

3.2 Artificial Images

Figure 5 shows two examples of the grouping process. In each case the left-hand image is the test pattern with the different eigenmodes coded with different colours The right-hand image is the set of lines belonging to the principal eigencluster (i.e. the one with the largest eigenvalue). In the first example (the top row), we show that the method is able to group the four central line-segments without connecting them to the three distractors. In the second example (the bottom row) the two crosses form distinct clusters and the principal eigencluster is the inner-most set of lines.

Figure 6 shows examples of the grouping process applied to an approximately circular configuration of line-segments. Here we have gradually added an increasing number of distractors to the figure. In each case the left-hand image of each pair shows the original line-pattern, whiel the right-hand image shows the cluster associated with the largest eigenvalue. The method does not break untill there are 400 distractors.

It is important to stress that the threshold ϵ has been set automatically in each of the examples presented in this section. In each case it adjusts itself to extract the dominant

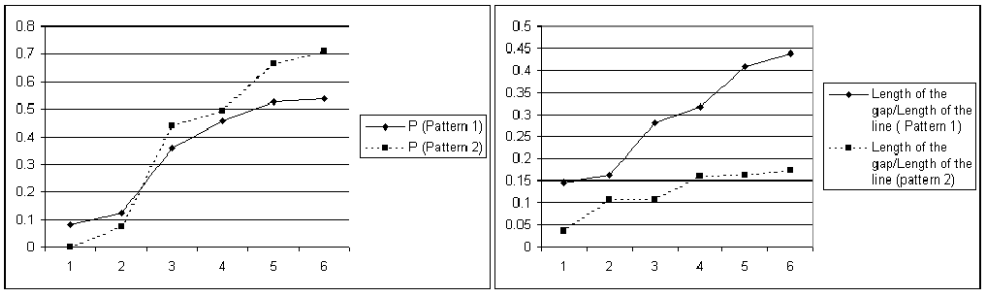

Figure 4: Results of the tests

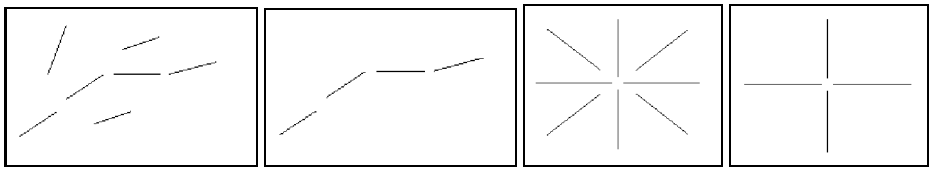

(a) (b) (c) (d)

Figure 5: (a) First line pattern; (b) Resulting cluster of the first line pattern; (c) Second line pattern; (d) Resulting cluster for the second line pattern

perceptual structure from the background. Finally, it is important to note that the eigen-clusters have been extracted using a single pass of the algorithm.

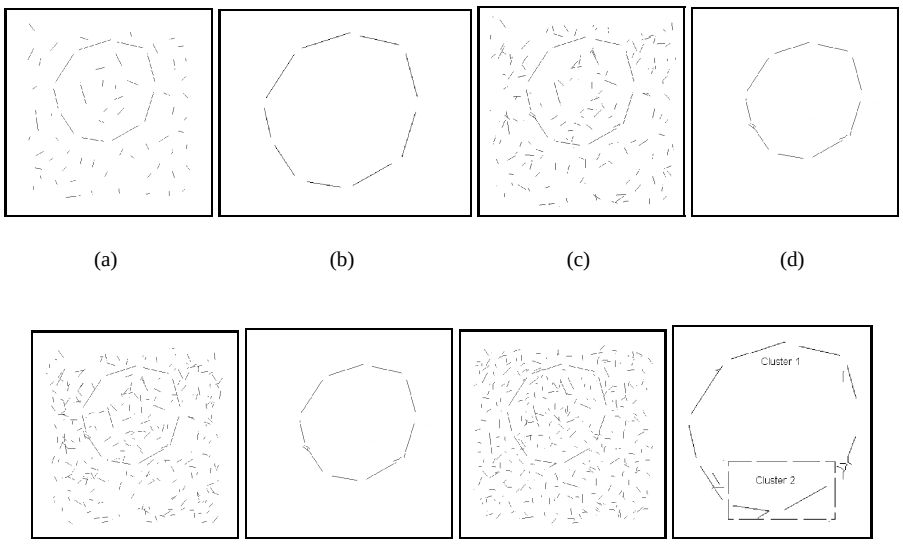

(a) (b) (c) (d)

(e) (f) (g) (h)

Figure 6: (a)Circular pattern with 100 distractors; (b) Resultant single cluster image; (c)Circular pattern with 100 distractors; (d) Resultant single cluster image; (e)Circular pattern with 300 distractors; (f) Resultant single cluster image; (g) Circular pattern too corrupted to be recognized(400 distractors); (h) Resultant pattern splited in two clusters

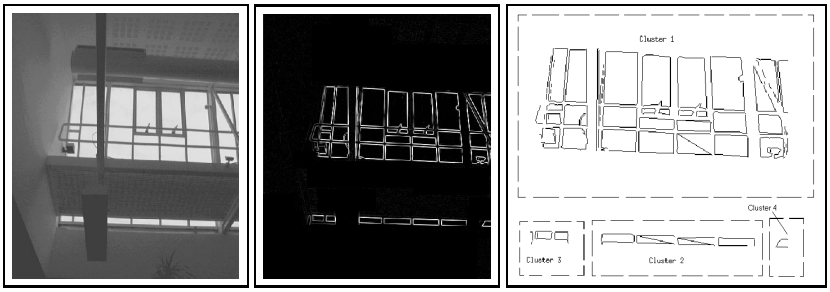

(a) (b) (c)

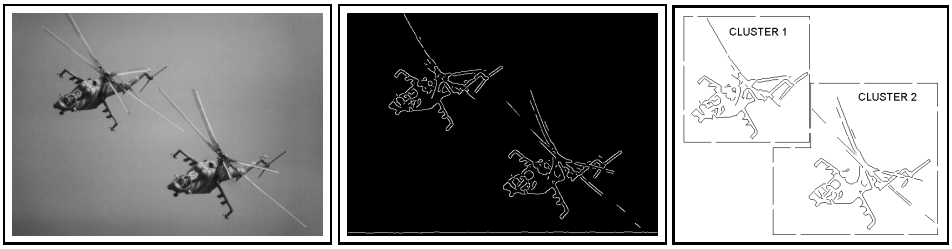

(d) (e) (f)

Figure 7: (a) Input image; (b) Result of the Canny Edge Detector; (c) Resulting cluster of the first image ($\epsilon = 0.17$); (d) Second input image; (e) Result of the Canny Edge Detector; (f) Resulting clusters ($\epsilon = 0.2084$)

3.3 Real World Images

In this section we present results on real-world images. The edges have been extracted from the raw images using the Canny edge-detector. Straight-line segments have been extracted using the method of Yin [4]. The different eigenclusters are again displayed in different colours.

In Figure 7a we show a cluttered image of the loft space above our lab. Figure 7b shows the edges extracted using the Canny edge-detector. Figure 7c shows the grouped line-segments. The different clusters correspond to distinct groups of lines. For instance even though the window is occluded by a beam, the set of glazing bars emerges as a single cluster.

The second image shown in Figure 7d showsis of two helicopters. Here the first two eigenclusters correspond to the two objects in the scene.

4 Conclusions

We have made three contributions in this paper. First we have described how to compute a line-linking field using a polar envelope. Second, we have shown how to automatically threshold the resulting field to produce a line-adjacency matrix. Finally, and most importantly we have developed a single-pass method for grouping the line-segments using the eigenvalues of the resulting adjacency matrix.

The grouping method offers a number of advantages, First the method appears to be capable of robustly linking straight when significant levels of noise and occlusion are present. Second, the method is capable of overcoming corner drop-out and works well with a variety of edge-detectors.

We plan to develop the work in a number of ways. First, we intend to extend the method to unthresholded proximity matrices. Second, we are exploring its use in conjunction with splines rather than straight-line segments.

References

[1] M. Doob D. Cvetković and H. Sachs. *Spectra of Graphs:Theory and Application*. Academic Press, 1980.

[2] G. Guy and G. Mendioni. Inferring global perceptual contours from local features. *International Journal of Computer Vision*, 20(1/2):113–133, 1996.

[3] F. Heitger and R. von der Heydt. A computational model of neural contour processing. In *IEEE CVPR*, pages 32–40, 1993.

[4] Yin Peng-Yeng. Algorithms for straight line fitting using k-means. *Pattern Recognition Letters*, 19:31–41, 1998.

[5] P. Perona and W. T. Freeman. Factorization approach to grouping. In *ECCV*, pages 655–670, 1998.

[6] S. Soltani P. K. Sahoo and A. K. C. Wong. A survey of thresholding techniques. *Comput. Vision, Graphics and Image Process.*, 41:233–260, 1988.

[7] S. Sarkar and K. L. Boyer. Quantitative measures of change based on feature organization: Eigenvalues and eigenvectors. *Computer Vision and Image Understanding*, 71(1):110–136, 1998.

[8] A. Shashua and S. Ullman. Structural saliency: The detection of globally salient structures using a locally connected network. In *Proc. 2nd Int. Conf. in Comp. Vision*, pages 321–327, 1988.

[9] J. Shi and J. Malik. Normalized cuts and image segmentations. In *CVPR*, pages 731–737, 1997.

[10] R.S. Varga. *Matrix Iterative Analysis*. Prentice Hall, 1962.

[11] J. S. Weszka. A survey of threshold selection techniques. *Computer Graphics and Image Processing*, 7:259–265, 1978.

[12] L. R. Williams and D. W. Jacobs. Local parallel computation of stochastic completion fields. *Neural Computation*, 9(4):859–882, 1997.

[13] L. R. Williams and D. W. Jacobs. Stochastic completion fields: A neural model of illusory contour shape and salience. *Neural Computation*, 9(4):837–858, 1997.